

Tunneling between two systems of interacting chiral fermions

D. B. Karki and K. A. Matveev

Materials Science Division, Argonne National Laboratory, Argonne, Illinois 60439, USA



(Received 22 October 2023; accepted 1 April 2024; published 12 April 2024)

We develop a theory of tunneling between two systems of spinless chiral fermions. This setup can be realized at the edge of a quantum Hall bilayer structure. We find that the differential conductance of such a device in the absence of interactions has an infinitely sharp peak as a function of applied voltage. Interaction between fermions results in broadening of the conductance peak. We focus on the regime of strong interactions, in which the shape of the peak manifests well defined features associated with the elementary excitations of the system.

DOI: [10.1103/PhysRevB.109.155415](https://doi.org/10.1103/PhysRevB.109.155415)

I. INTRODUCTION

Interactions between one-dimensional fermions give rise to a number of strongly correlated phenomena [1]. Their complete understanding is generally beyond the scope of the Landau Fermi liquid paradigm [2]. Instead, the low-energy properties of one-dimensional systems are typically described in terms of the Luttinger liquid theory [3]. The best known feature of this theory is the power-law scaling of the tunneling density of states at low energies [4,5]. Luttinger liquid behavior has been experimentally observed in various one-dimensional systems, such as carbon nanotubes [6–8] and semiconductor quantum wires [9].

Similar phenomena have been predicted to emerge at the edges of fractional quantum Hall systems [10,11]. In this case, the low energy excitations are described by the chiral Luttinger liquid theory, in which the properties of the system are controlled by the filling fraction ν of the corresponding quantum Hall state. For ν^{-1} being an odd integer, the tunneling density of states of the chiral Luttinger liquid was predicted to follow the power-law behavior $D(\epsilon) \propto \epsilon^\chi$, where ϵ is the energy measured from the chemical potential and $\chi = \nu^{-1} - 1$ [10]. These predictions have been confirmed experimentally [12,13]. We note that although the very existence of fractional quantum Hall effect and, therefore, chiral Luttinger liquid at its edge, is due to the electron-electron interactions; the exponent in the above power law does not explicitly depend on the interaction strength.

In this work we consider the special case of integer quantum Hall effect with filling factor $\nu = 1$. The edge state of this system can be modeled as a system of chiral one-dimensional fermions [14]. At $\nu = 1$, the above power law gives a finite tunneling density of states at the chemical potential. Therefore, one may assume that the interactions do not significantly affect the properties of one-dimensional chiral fermions. On the other hand, recent work on spinless chiral fermions shows that the effects of interactions manifest themselves in the behavior of the spectral function of the system [15]. In particular, at fixed momentum p , the spectral function $A_p(\epsilon)$ has the shape of a peak with the width proportional to the interaction strength.

The main difference between the density of states $D(\epsilon)$ and the spectral function $A_p(\epsilon)$ is that the latter describes the

response of the system when a particle is added to or removed from it has a fixed momentum p . In one dimension, such physical processes can be probed experimentally in devices with momentum-conserved tunneling setup [16–20]. In recent experiments [21,22], momentum-conserved tunneling between a quantum wire and a quantum Hall system was used to probe the edge states with unprecedented accuracy. Alternatively, momentum-conserved tunneling can be achieved in quantum Hall bilayer devices [23–26] operated in the regime, where transport between the layers is dominated by edge states rather than the gapped excitations in the bulk. Given these experimental advances, it is important to study theoretically how interactions affect momentum-conserved tunneling in systems of interacting chiral fermions.

In this paper, we develop a general theory of momentum-conserved tunneling between two systems of spinless one-dimensional chiral fermions. We account for interactions both within and between the two systems and focus on the limit of strong interactions. As an application of our theory, we study tunneling between the edge states in a quantum Hall bilayer device. We show that the differential conductance of such a device has a sharp peak as a function of applied voltage. We find that the shape of the peak shows well defined features associated with the elementary excitations of the system.

II. MODEL

We consider two systems of interacting one-dimensional spinless chiral fermions separated by a short distance, as illustrated in Fig. 1(a). This setup is described by the Hamiltonian $\hat{H} = \hat{H}_0 + \hat{H}_T$, with

$$\begin{aligned} \hat{H}_0 = & \sum_p \epsilon_p^{(1)} c_{1,p}^\dagger c_{1,p} + \sum_p \epsilon_p^{(2)} c_{2,p}^\dagger c_{2,p} \\ & + \frac{1}{L} \sum_{j=1}^2 \sum_{\substack{pp' \\ q>0}} V^{(j)}(q) c_{j,p+q}^\dagger c_{j,p} c_{j,p'}^\dagger c_{j,p'+q} \\ & + \frac{1}{L} \sum_{\substack{pp' \\ q>0}} \tilde{V}(q) (c_{1,p+q}^\dagger c_{1,p} c_{2,p'}^\dagger c_{2,p'+q} \\ & + c_{2,p+q}^\dagger c_{2,p} c_{1,p'}^\dagger c_{1,p'+q}). \end{aligned} \quad (1)$$

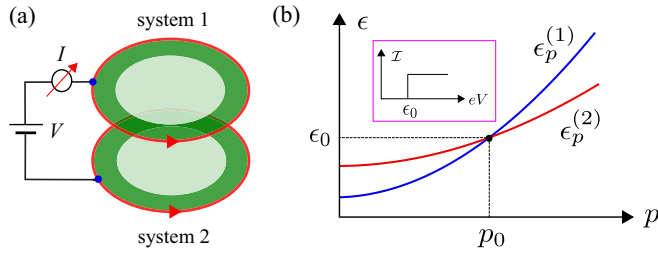


FIG. 1. (a) The schematic representation of the setup under consideration, which can be realized in quantum Hall bilayer devices. (b) The sketch of the free fermion dispersions $\epsilon_p^{(j)}$. In the absence of interactions, current shows steplike behavior as illustrated in the inset.

Here the operator $c_{j,p}$ annihilates a fermion in the state with momentum p in system j , with $j = 1, 2$. The energy of fermions in system j is represented by $\epsilon_p^{(j)}$, which is assumed to be a monotonic function of p . Motivated by the experiments on quantum Hall bilayer devices, we assume that the two systems of chiral fermions are of the same length L and have similar properties, but are not identical. The interactions within each system and between them are expressed in terms of the Fourier transformed interaction potentials $V^{(j)}(q)$ and $\tilde{V}(q)$, respectively. In this paper, we assume that these quantities are positive, which corresponds to repulsive interactions. The operator

$$\hat{H}_T = \sum_p (\gamma_p c_{1,p}^\dagger c_{2,p} + \gamma_p^* c_{2,p}^\dagger c_{1,p}) \quad (2)$$

describes momentum-conserved tunneling between the two systems; γ_p stands for the tunneling matrix element.

To calculate the tunneling current, we start with the operator $\hat{I} = (ie/\hbar) \sum_p (\gamma_p c_{1,p}^\dagger c_{2,p} - \text{H.c.})$ accounting for the charge current from system 1 to system 2. Assuming a weak tunneling regime, we proceed with the evaluation of charge current $\langle \hat{I} \rangle$ perturbatively in \hat{H}_T and, retaining only the terms of the lowest order in γ_p . The resulting expression for the current per unit length $\mathcal{I} = \langle \hat{I} \rangle / L$ takes the form

$$\mathcal{I} = \frac{e}{L\hbar^2} \sum_p |\gamma_p|^2 \int_{-\infty}^{\infty} dt [\mathcal{F}_p^{(12)}(t) - \mathcal{F}_p^{(21)}(-t)], \quad (3a)$$

$$\mathcal{F}_p^{(jj)}(t) = \langle c_{j,p}^\dagger(t) c_{j',p}(t) c_{j',p}^\dagger(0) c_{j,p}(0) \rangle. \quad (3b)$$

In the absence of interactions, the two particle average (3b) decouples into the product of single particle averages, which can be calculated straightforwardly. In this case, Eq. (3a) gives the expression for current per unit length at zero temperature in the form

$$\mathcal{I} = \frac{e}{\hbar^2} \sum_m |\gamma_{p_m}|^2 \frac{[\theta(\epsilon_m - \mu_2) - \theta(\epsilon_m - \mu_1)]}{|\partial_p(\epsilon_p^{(1)} - \epsilon_p^{(2)})|_{p=p_m}}, \quad (4)$$

where $\theta(x)$ is the unit step function and μ_j stands for the chemical potential of the system j . Momentum-conserved tunneling is possible when the energies of fermions in two systems become equal at a certain momentum, i.e., $\epsilon_p^{(1)} = \epsilon_p^{(2)}$. In general, there are several solutions $p = p_m$ of this equation; the corresponding energies are denoted by ϵ_m , where

$m = 0, 1, \dots$. Figure 1(b) illustrates the case of a single solution with $p = p_0$.

To study the current-voltage characteristic of the device, we introduce voltage as $eV = \mu_1 - \mu_2$ and also assume that the chemical potential μ_2 is fixed and chosen as the origin of energy, i.e., $\mu_2 = 0$. The current (4) shows steps as a function of voltage. Current-voltage characteristics in the case of a single solution with $\epsilon_p^{(1)} = \epsilon_p^{(2)} = \epsilon_0 > 0$ is shown in the inset of Fig. 1(b). The corresponding differential conductance per unit length $G = \partial \mathcal{I} / \partial V$ has an infinitely sharp peak at $eV = \epsilon_0$.

The main objective of this work is to investigate how the presence of strong interactions within and between the systems affects the current-voltage characteristic shown in the inset of Fig. 1(b). In this case, the average (3b) no longer decouples. We focus on the low energy regime, where calculations in the presence of strong interactions are simplified greatly upon the bosonization of the Hamiltonian of the system.

III. BOSONIZATION

We follow the standard bosonization procedure [3] to reformulate the problem in bosonic variables using the transformation

$$\psi_j(x) = \frac{\hat{u}_j}{\sqrt{L}} e^{ip_F^{(j)}x/\hbar} e^{i\varphi_j^\dagger(x)} e^{i\varphi_j(x)}. \quad (5)$$

Here $\psi_j(x)$ annihilates a fermion at position x in system j ; it is related to the operator $c_{j,p}$ by the Fourier transformation. The operator \hat{u}_j lowers the particle number N_j in system j by one, i.e., $[\hat{u}_j, \hat{N}_j] = \hat{u}_j$, and also includes the Klein factor emerging in the bosonization procedure. The Fermi momentum of system j is denoted by $p_F^{(j)}$. The bosonic fields $\varphi_j(x)$ are defined by

$$\varphi_j(x) = -i \sum_{l=1}^{\infty} \frac{1}{\sqrt{l}} e^{iq_l x/\hbar} b_{j,l}, \quad q_l = \frac{2\pi\hbar}{L} l, \quad (6)$$

with $b_{j,l}$ being the bosonic annihilation operators.

To express \hat{H}_0 in terms of bosonic variables, we first note that in the strong interaction regime, the curvature of electronic dispersion can be neglected [15]. Thus, we linearize the fermion dispersion $\epsilon_p^{(j)}$ near the Fermi point,

$$\epsilon_p^{(j)} = \mu_j + v_F^{(j)}(p - p_F^{(j)}), \quad (7)$$

where the corresponding Fermi velocity is denoted by $v_F^{(j)}$. We note that the Fermi momentum $p_F^{(j)}$ depends on the chemical potential μ_j and that this dependence is affected by the interactions [27]. Using Eqs. (5)–(7), we express the operator \hat{H}_0 in terms of bosonic variables as

$$\begin{aligned} \hat{H}_0 = & \sum_{l=1}^{\infty} (\epsilon_l^{(1)} b_{1,l}^\dagger b_{1,l} + \epsilon_l^{(2)} b_{2,l}^\dagger b_{2,l}) + \mu_1 \hat{N}_1 + \mu_2 \hat{N}_2 \\ & + \sum_{l=1}^{\infty} U_l (b_{1,l}^\dagger b_{2,l} + b_{2,l}^\dagger b_{1,l}), \end{aligned} \quad (8a)$$

$$\epsilon_l^{(j)} = \left[v_F^{(j)} + \frac{V^{(j)}(q_l)}{2\pi\hbar} \right] q_l, \quad U_l = \frac{\tilde{V}(q_l)}{2\pi\hbar} q_l. \quad (8b)$$

It is convenient to bring Eq. (8a) to the diagonal form

$$\hat{H}_0 = \sum_{l=1}^{\infty} (\tilde{\varepsilon}_l^{(1)} \tilde{b}_{1,l}^\dagger \tilde{b}_{1,l} + \tilde{\varepsilon}_l^{(2)} \tilde{b}_{2,l}^\dagger \tilde{b}_{2,l}) + \mu_1 \hat{N}_1 + \mu_2 \hat{N}_2 \quad (9)$$

by performing the transformation

$$\begin{pmatrix} b_{1,l} \\ b_{2,l} \end{pmatrix} = \begin{pmatrix} \cos \theta_l & -\sin \theta_l \\ \sin \theta_l & \cos \theta_l \end{pmatrix} \begin{pmatrix} \tilde{b}_{1,l} \\ \tilde{b}_{2,l} \end{pmatrix}, \quad \tan 2\theta_l = \frac{2U_l}{\varepsilon_l^{(1)} - \varepsilon_l^{(2)}}. \quad (10)$$

The energies $\tilde{\varepsilon}_l^{(j)}$ in Eq. (9) are defined by

$$\tilde{\varepsilon}_l^{(j)} = \frac{\varepsilon_l^{(1)} + \varepsilon_l^{(2)}}{2} - \frac{(-1)^j}{2} \sqrt{(\varepsilon_l^{(1)} - \varepsilon_l^{(2)})^2 + 4U_l^2}, \quad (11)$$

where we assumed $\varepsilon_l^{(1)} > \varepsilon_l^{(2)}$ [28].

IV. EXPRESSION FOR THE CHARGE CURRENT

To evaluate the charge current (3a), we need an expression for the time dependent operator $\psi_j(x, t)$. In addition to the time dependence of the bosonic field φ_j in Eq. (5), the Hamiltonian (9) generates the time dependence of the lowering operator $\hat{u}_j(t) = \hat{u}_j e^{-i\mu_j t/\hbar}$. Therefore,

$$\psi_j(x, t) = \frac{\hat{u}_j}{\sqrt{L}} e^{-i\mu_j t/\hbar} e^{ip_F^{(j)} x/\hbar} e^{i\varphi_j^\dagger(x,t)} e^{i\varphi_j(x,t)}. \quad (12)$$

Using Eqs. (3a) and (12), we proceed with the evaluation of charge current. In the thermodynamic limit $L \rightarrow \infty$, we find the following expression for the current per unit length at zero temperature [27]:

$$\mathcal{I} = \frac{e|\gamma|^2}{\hbar^2} \int_{-\infty}^{\infty} dq \int_{-\infty}^{\infty} d\varepsilon \tilde{A}^{(1)}(q, \varepsilon) \times \tilde{A}^{(2)}(\Delta p_F - q, \Delta\mu - \varepsilon). \quad (13)$$

Here $\Delta p_F = p_F^{(1)} - p_F^{(2)}$ and $\Delta\mu = \mu_1 - \mu_2 > 0$. At low energies, tunneling of fermions is confined to the vicinity of the Fermi level, and thus to arrive at Eq. (13) we neglected the momentum dependence of the tunneling matrix element, $\gamma_p \rightarrow \gamma$. The function $\tilde{A}^{(j)}$ is defined by

$$\tilde{A}^{(j)}(q, \varepsilon) = \lim_{L \rightarrow \infty} \int_{-\infty}^{\infty} \frac{dt}{2\pi\hbar} \int_0^L \frac{dy}{L} e^{-i(qy - \varepsilon t)/\hbar} \times \exp\left(\sum_{l=1}^{\infty} \frac{1}{l} e^{i[qly - \tilde{\varepsilon}^{(j)}(q_l)t]/\hbar}\right). \quad (14)$$

We note that, in the absence of interactions between the two systems, $\tilde{A}^{(j)}$ represents the spectral function of the system j [15]. In this case, the charge current given by Eq. (13) is proportional to the convolution of the spectral functions of the two systems.

The form of the charge current given by Eq. (13) reflects the momentum and energy conservation in our system. To demonstrate this, we consider a process of tunneling of fermions from system 1 to system 2. This particle exchange process produces the overall change in the energy of the system $\varepsilon_1 + \varepsilon_2 - \Delta\mu$ as seen from Eq. (9). Here, ε_j is the total energy of bosonic excitations in the branch j after tunneling.

Similarly, the change in momentum is $q_1 + q_2 - \Delta p_F$, with q_j being the total momentum of the bosonic branch j . Therefore, the conservation of energy and momentum requires $\varepsilon_2 = \Delta\mu - \varepsilon_1$ and $q_2 = \Delta p_F - q_1$, which is reflected in Eq. (13). To study the current (13) in more detail, we need to specify a particular form of the interactions.

V. CONTACT INTERACTIONS

In the limit of extremely short range interactions, the energy of bosonic excitations given in Eq. (11) is linear in momentum, i.e., $\tilde{\varepsilon}^{(j)}(q) = \tilde{v}_j q$, where

$$\tilde{v}_{1,2} = \frac{v_1 + v_2 \pm \sqrt{(v_1 - v_2)^2 + 4v_{12}^2}}{2}, \quad (15a)$$

$$v_j = v_F^{(j)} + \frac{V^{(j)}(0)}{2\pi\hbar}, \quad v_{12} = \frac{\tilde{V}(0)}{2\pi\hbar}. \quad (15b)$$

To study the charge current (13), we also need an expression for the voltage dependence of Δp_F . Setting again $\mu_1 = eV$ and $\mu_2 = 0$, we obtain [27]

$$\Delta p_F(V) = \Delta p_F(0) + \frac{eV}{\bar{v}}, \quad \bar{v} = \frac{v_1 v_2 - v_{12}^2}{v_2 + v_{12}}. \quad (16)$$

For the linear dispersion $\tilde{\varepsilon}^{(j)}(q) = \tilde{v}_j q$, Eq. (14) yields $\tilde{A}^{(j)}(q, \varepsilon) = \theta(\varepsilon) \delta(\varepsilon - \tilde{v}_j q)$. Using Eq. (13), we then find

$$\mathcal{I} = \frac{e|\gamma|^2}{\hbar^2(\tilde{v}_1 - \tilde{v}_2)} [\theta(eV - eV_1) + \theta(eV - eV_2) - 1], \quad (17)$$

where V_j is found from the condition $eV_j = \tilde{v}_j \Delta p_F(V_j)$, and is given by $eV_j = \tilde{v}_j \bar{v} \Delta p_F(0) / (\bar{v} - \tilde{v}_j)$. Although Eq. (13) was written for $\Delta\mu > 0$, the result (17) applies for both positive and negative voltage V .

In general, the charge current (17) has two steps positioned at the voltages V_j , with V_1 and V_2 being of the opposite sign due the inequality $\tilde{v}_1 \geq \bar{v} \geq \tilde{v}_2$. At small $\Delta p_F(0)$, voltages V_1 and V_2 are small and thus we are in the regime of applicability of bosonization theory. The number of steps reduces to one in two special cases. First, in the absence of interactions between the two systems, i.e., $\tilde{V}(0) = 0$ and thus $v_{12} = 0$, we have $V_1 \rightarrow \infty$. Second, in the limit of $v_1 = v_2$, we get $V_2 \rightarrow \infty$.

It is instructive to compare this behavior with that of noninteracting systems, where current is given by Eq. (4). Assuming linear dispersions in Eq. (4), we find only one step. The absence of the second step is due to the fact that the applied voltage changes only $p_F^{(1)}$, while $p_F^{(2)}$ is fixed. Different application of voltage, such as $\mu_{1,2} = \pm eV/2$, would result in two steps in $\mathcal{I}(V)$. In the special case, when the Fermi velocities of the two systems are identical, current (4) vanishes. This is in contrast to the case of interacting systems, where even at $v_1 = v_2$, current (17) yields a step at voltage V_1 .

VI. SHORT RANGE INTERACTIONS

When the range of interactions is nonzero, the nonlinearity of the bosonic spectrum should be taken into account. Assuming the interactions are of short range, we substitute $\varepsilon^{(j)}(q) = v_j q - \eta_j q^3 / (2\pi\hbar)$ and $U(q) = v_{12} q - \eta_{12} q^3 / (2\pi\hbar)$ into Eq. (11) and obtain the bosonic spectra $\tilde{\varepsilon}^{(j)}$

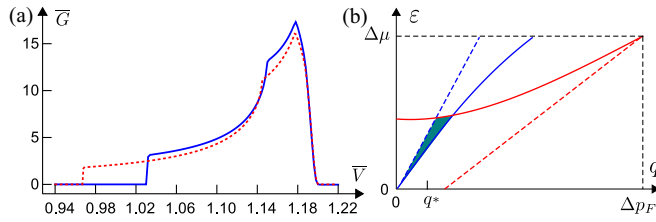


FIG. 2. (a) The dimensionless form of differential conductance defined by $\bar{G} = \partial \bar{\mathcal{I}} / \partial \bar{V}$, where $\bar{\mathcal{I}} = (\hbar^2 v_1 / e |\gamma|^2) \mathcal{I}$ and $\bar{V} = eV / [\Delta p_F(0) v_1]$. The solid blue curve is obtained from Eq. (13) for the choice of parameters $v_2 = 0.5v_1$, $v_{12} = 0.3v_1$, $\eta_2 = 0.8\eta_1$, $\eta_{12} = 0.6\eta_1$, and $\eta_1 [\Delta p_F(0)]^2 / (2\pi \hbar v_1) = 0.005$. The dotted red curve shows the conductance to leading order in small nonlinearity given by Eq. (20) for the same values of parameters as that of the blue curve. (b) The blue and red lines are the plots of the spectra $\tilde{\varepsilon}_1(q)$ and $\Delta\mu - \tilde{\varepsilon}_2(\Delta p_F - q)$. Dashed lines show the linear asymptotes of corresponding bosonic spectra. Only the small shaded triangular region with typical momentum q^* contributes to the current (13).

in the form

$$\tilde{\varepsilon}^{(j)}(q) = \tilde{v}_j q - \frac{\tilde{\eta}_j}{2\pi \hbar} q^3. \quad (18)$$

Here the parameter $\tilde{\eta}_j > 0$ accounts for the curvature of the bosonic spectrum; its expression in terms of microscopic parameters of the model is given in Ref. [27]. For the spectrum (18), the function $\tilde{A}^{(j)}$ takes the form [15]

$$\tilde{A}^{(j)}(q, \varepsilon) = \frac{2\pi \hbar}{\tilde{\eta}_j q^3} a\left(\frac{2\pi \hbar}{\tilde{\eta}_j q^3} [\varepsilon - \tilde{\varepsilon}^{(j)}(q)]\right). \quad (19)$$

Here $a(x)$ is a universal function, which vanishes outside the region $0 < x < 1$ and has singularities at $x = 1 - n^{-2}$, where $n = 1, 2, \dots$. The position of the n th singularity corresponds to the energy $\varepsilon = n\tilde{\varepsilon}^{(j)}(q/n)$ and thus reflects the nature of the many-body excitations in the system.

Substitution of Eq. (19) into Eq. (13) allows one to study the differential conductance per unit length $G = \partial \mathcal{I} / \partial V$ for $\Delta\mu = eV > 0$. Thus, assuming $\Delta p_F(0) > 0$, we now study the differential conductance in the vicinity of the step at $V = V_2$. For a particular choice of parameters, the voltage dependence $G(V)$ obtained numerically from Eq. (13) is plotted in Fig. 2(a). The δ -function peak of conductance in the case of contact interactions is now broadened because of the nonlinearity of the bosonic spectrum. The shape of the peaks shows clear singularities at certain values of voltage.

To understand the shape of the peak of differential conductance shown in Fig. 2(a), we study the current (13) in leading order in small parameters $\tilde{\eta}_j$. To this end, we first note that the function $\tilde{A}^{(j)}(q, \varepsilon)$ defined by Eq. (14) is finite only when both momentum and energy are positive. This constraint restricts the range of integration in Eq. (13) to $0 < q < \Delta p_F$ and $0 < \varepsilon < \Delta\mu$, which corresponds to the rectangle shown in Fig. 2(b). In addition, the concavity of spectrum (18) guarantees that the total energy ε_j of any set of bosonic excitations with the total momentum q is in the range $\tilde{\varepsilon}^{(j)}(q) \leq \varepsilon_j < \tilde{v}_j q$. [This is the reason why $a(x)$ in Eq. (19) vanishes outside the region $0 < x < 1$]. It is then clear that only the region defined by $\tilde{\varepsilon}^{(1)}(q) \leq \varepsilon < \tilde{v}_1 q$ and

$\Delta\mu - \tilde{\varepsilon}^{(2)}(\Delta p_F - q) \geq \varepsilon > \Delta\mu - \tilde{v}_2(\Delta p_F - q)$ contributes to the current (13). This region can be visualized by plotting the spectra $\tilde{\varepsilon}^{(1)}(q)$ and $\Delta\mu - \tilde{\varepsilon}^{(2)}(\Delta p_F - q)$ along with their linear asymptotes as illustrated in Fig. 2(b), where we took $\Delta\mu \sim eV_2$, i.e., the red dotted line passes near the point $(q, \varepsilon) = (0, 0)$. From the figure, it is seen that only the small triangular region formed by crossing of the spectrum of the slow branch (red) with that of the fast branch (blue) and its linear asymptote (dashed blue) contributes to the current (13).

In the case of weak nonlinearity, i.e., $(\Delta p_F)^2 \tilde{\eta}_j \ll 2\pi \hbar \tilde{v}_j$, typical momentum q^* within this triangular region is small, $q^* \ll \Delta p_F$. Thus, the broadening of $\tilde{A}^{(1)}(q, \varepsilon)$ due to the nonlinearity of spectrum can be neglected compared to that of $\tilde{A}^{(2)}(\Delta p_F - q, \Delta\mu - \varepsilon)$, i.e., we can replace $\tilde{A}^{(1)}(q, \varepsilon) \rightarrow \theta(\varepsilon) \delta(\varepsilon - \tilde{v}_1 q)$. Equation (13) then reduces to a single integral. The result to leading order in $\tilde{\eta}_2$ takes the compact form [29]

$$\mathcal{I} = \frac{e|\gamma|^2}{\hbar^2(\tilde{v}_1 - \tilde{v}_2)} \int_0^{1+\lambda} dx a(x), \quad (20a)$$

$$\lambda = \frac{2\pi \hbar e(V - V_2)}{\tilde{\eta}_2 [\Delta p_F(0)]^3} \left(1 - \frac{\tilde{v}_2}{\tilde{v}_1}\right)^4. \quad (20b)$$

Current (20) vanishes at voltages corresponding to $\lambda < -1$, then grows monotonically and reaches a plateau at voltage V_2 , where λ vanishes. Differentiation of Eq. (20) with respect to voltage yields a conductance peak with the shape essentially identical to that of the universal function $a(x)$. As shown in Fig. 2(a), the differential conductance obtained from Eq. (20) reproduces all the features of that obtained from Eq. (13) numerically.

VII. DISCUSSION

Our results can be tested in experiments with quantum Hall bilayer structures. The sizes of the devices in the existing experiments [23–26] are large, and as a result the transport is dominated by the gapped excitations in the bulk. By using smaller size structures, transport properties dominated by the edge states can be investigated. Typically, in quantum Hall devices, the electron density is controlled by nearby gates, which screen the Coulomb interactions and thus the case of short range interactions discussed here will be relevant. A small temperature and disorder are expected to result in broadening of the sharp features shown in Fig. 2.

To summarize, we presented a low-energy theory of momentum-conserved tunneling between two systems of spinless one-dimensional chiral fermions in the regime of strong interactions. We applied our theory to study transport in small quantum Hall bilayer devices. We showed that the differential conductance of such a device has a distinctive shape with nontrivial features reflecting the many-body physics of interacting chiral fermions.

ACKNOWLEDGMENT

This work was supported by the U.S. Department of Energy, Office of Science, Basic Energy Sciences, Materials Sciences and Engineering Division.

- [1] T. Giamarchi, *Quantum Physics in One Dimension*, International Series of Monographs on Physics (Clarendon Press, Oxford, 2004).
- [2] D. Pines and P. Nozières, *The Theory of Quantum Liquids: Normal Fermi Liquids* (CRC Press, Boca Raton, 2019), Vol. 1.
- [3] F. D. M. Haldane, ‘Luttinger liquid theory’ of one-dimensional quantum fluids. I. Properties of the Luttinger model and their extension to the general 1D interacting spinless Fermi gas, *J. Phys. C* **14**, 2585 (1981).
- [4] C. L. Kane and M. P. A. Fisher, Transmission through barriers and resonant tunneling in an interacting one-dimensional electron gas, *Phys. Rev. B* **46**, 15233 (1992).
- [5] A. Furusaki and N. Nagaosa, Resonant tunneling in a Luttinger liquid, *Phys. Rev. B* **47**, 3827 (1993).
- [6] M. Bockrath, D. H. Cobden, J. Lu, A. G. Rinzler, R. E. Smalley, L. Balents, and P. L. McEuen, Luttinger-liquid behavior in carbon nanotubes, *Nature (London)* **397**, 598 (1999).
- [7] B. Gao, A. Komnik, R. Egger, D. C. Glattli, and A. Bachtold, Evidence for Luttinger-liquid behavior in crossed metallic single-wall nanotubes, *Phys. Rev. Lett.* **92**, 216804 (2004).
- [8] H. Ishii, H. Kataura, H. Shiozawa, H. Yoshioka, H. Otsubo, Y. Takayama, T. Miyahara, S. Suzuki, Y. Achiba, M. Nakatake, T. Narimura, M. Higashiguchi, K. Shimada, H. Namatame, and M. Taniguchi, Direct observation of Tomonaga-Luttinger-liquid state in carbon nanotubes at low temperatures, *Nature (London)* **426**, 540 (2003).
- [9] E. Levy, A. Tsukernik, M. Karpovski, A. Palevski, B. Dwir, E. Pelucchi, A. Rudra, E. Kapon, and Y. Oreg, Luttinger-liquid behavior in weakly disordered quantum wires, *Phys. Rev. Lett.* **97**, 196802 (2006).
- [10] X.-G. Wen, Theory of the edge states in fractional quantum Hall effects, *Int. J. Mod. Phys. B* **06**, 1711 (1992).
- [11] X.-G. Wen, Topological orders and edge excitations in fractional quantum Hall states, *Adv. Phys.* **44**, 405 (1995).
- [12] A. M. Chang, L. N. Pfeiffer, and K. W. West, Observation of chiral Luttinger behavior in electron tunneling into fractional quantum Hall edges, *Phys. Rev. Lett.* **77**, 2538 (1996).
- [13] A. M. Chang, Chiral Luttinger liquids at the fractional quantum Hall edge, *Rev. Mod. Phys.* **75**, 1449 (2003).
- [14] B. I. Halperin, Quantized Hall conductance, current-carrying edge states, and the existence of extended states in a two-dimensional disordered potential, *Phys. Rev. B* **25**, 2185 (1982).
- [15] K. A. Matveev, Spectral function of the chiral one-dimensional Fermi liquid in the regime of strong interactions, *Phys. Rev. Lett.* **128**, 176802 (2022).
- [16] W. Kang, H. L. Stormer, L. N. Pfeiffer, K. W. Baldwin, and K. W. West, Tunneling between the edges of two lateral quantum Hall systems, *Nature (London)* **403**, 59 (2000).
- [17] O. M. Auslaender, A. Yacoby, R. de Picciotto, K. W. Baldwin, L. N. Pfeiffer, and K. W. West, Tunneling spectroscopy of the elementary excitations in a one-dimensional wire, *Science* **295**, 825 (2002).
- [18] Y. Tserkovnyak, B. I. Halperin, O. M. Auslaender, and A. Yacoby, Finite-size effects in tunneling between parallel quantum wires, *Phys. Rev. Lett.* **89**, 136805 (2002).
- [19] Y. Tserkovnyak, B. I. Halperin, O. M. Auslaender, and A. Yacoby, Interference and zero-bias anomaly in tunneling between Luttinger-liquid wires, *Phys. Rev. B* **68**, 125312 (2003).
- [20] H. Steinberg, G. Barak, A. Yacoby, L. N. Pfeiffer, K. W. West, B. I. Halperin, and K. L. Hur, Charge fractionalization in quantum wires, *Nat. Phys.* **4**, 116 (2008).
- [21] T. Patlatiuk, C. P. Scheller, D. Hill, Y. Tserkovnyak, G. Barak, A. Yacoby, L. N. Pfeiffer, K. W. West, and D. M. Zumbühl, Evolution of the quantum Hall bulk spectrum into chiral edge states, *Nat. Commun.* **9**, 3692 (2018).
- [22] T. Patlatiuk, C. P. Scheller, D. Hill, Y. Tserkovnyak, J. C. Egues, G. Barak, A. Yacoby, L. N. Pfeiffer, K. W. West, and D. M. Zumbühl, Edge-state wave functions from momentum-conserving tunneling spectroscopy, *Phys. Rev. Lett.* **125**, 087701 (2020).
- [23] J. P. Eisenstein, New transport phenomena in coupled quantum wells, *Superlattices Microstruct.* **12**, 107 (1992).
- [24] A. D. K. Finck, J. P. Eisenstein, L. N. Pfeiffer, and K. W. West, Exciton transport and Andreev reflection in a bilayer quantum Hall system, *Phys. Rev. Lett.* **106**, 236807 (2011).
- [25] X. Huang, W. Dietsche, M. Hauser, and K. von Klitzing, Coupling of Josephson currents in quantum Hall bilayers, *Phys. Rev. Lett.* **109**, 156802 (2012).
- [26] D. Nandi, T. Khaire, A. D. K. Finck, J. P. Eisenstein, L. N. Pfeiffer, and K. W. West, Tunneling at $\nu_T = 1$ in quantum Hall bilayers, *Phys. Rev. B* **88**, 165308 (2013).
- [27] See Supplemental Material at <http://link.aps.org/supplemental/10.1103/PhysRevB.109.155415> for the details.
- [28] The interaction parameters $V^{(j)}$ and $V^{(12)}$ are independent. In general, the interactions within the systems are stronger than those between the systems. Therefore, we proceed with the assumption $V^{(j)} > V^{(12)}$, which guarantees $\tilde{\xi}_i^{(1)} > \tilde{\xi}_i^{(2)} > 0$.
- [29] A better agreement with the numerical result shown in Fig. 2(a) is obtained when higher order corrections are taken into account [27].